Nonlinear corrections to Darcy's law at low Reynolds numbers

By MOUAOUIA FIRDAOUSS[1,2],
JEAN-LUC GUERMOND[1] AND PATRICK LE QUÉRÉ[1]

[1]LIMSI, CNRS, BP 133, 91403, Orsay, France
[2]UFR 23, UPMC Paris VI, Paris, France

Under fairly general assumptions, this paper shows that for periodic porous media, whose period is of the same order as that of the inclusion, the nonlinear correction to Darcy's law is quadratic in terms of the Reynolds number, i.e. cubic with respect to the seepage velocity. This claim is substantiated by reinspection of well-known experimental results, a mathematical proof (restricted to periodic porous media), and numerical calculations.

1. Introduction

The most popular filtration experiment is due to Darcy (1856). The result referred to as Darcy's law is that the flow rate of water through a filter bed is directly proportional to the area of the filter bed and to the pressure drop in the fluid and inversely proportional to the thickness of the bed, i.e. the seepage velocity is directly proportional to the pressure gradient, and this relation is usually written in the form

$$-\frac{1}{\mu}\boldsymbol{K}_0 \cdot \nabla p = \boldsymbol{u}. \qquad (1.1)$$

This law is now very well understood, and can be rigorously proven by means of the homogenization theory, either in the two-scale form developed by Sanchez-Palencia (1980) or by using the energy technique pioneered by Tartar (1980).

Many years after Darcy's historical experiment, other researchers found that some deviation from the above-mentioned proportionality law occurs as the seepage velocity increases. After Reynolds' landmark experiment and his unveiling of the nonlinear effects on fluid flows, it became clear that the relevant parameter in Darcy's experiment is not the seepage velocity but the Reynolds number that is based on it, and that the deviation from Darcy's law is induced by inertia effects.

Usually the flow through the porous medium is driven by a macroscopic pressure gradient $\Delta P/L$, where L is a macroscopic length scale. Inspection of the Stokes equations that control the flow between the grains of the porous medium gives the velocity scale: $a^2\Delta P/\mu L$, where a is a measure of the grain size or of the distance between the grains, or of any other length scale which is characteristic of the microscopic geometry, and μ is the dynamic viscosity. Note that this scaling of the velocity is correct only if the size of the grain is of order a, for a Poincaré inequality is involved as shown in Tartar (1980) or Allaire (1989). The microscopic (or local)

Reynolds number is defined as

$$R_e = \frac{\Delta P a^3 \rho}{L \mu^2}.$$

(1.2)

Adopting $\Delta P/L$ and $a^2 \Delta P/\mu L$ as characteristic scales for the pressure gradient and the velocity and using $\bar{u}, \bar{p}$ as scaled variables, one way of representing the nonlinear effects in dimensionless form is to assume some polynomial form

$$-\overline{\boldsymbol{K}}_0 \cdot \overline{\nabla p} = \bar{u} + R_e \overline{f}(\bar{u}, \bar{u}) + R_e^2 \overline{g}(\bar{u}, \bar{u}, \bar{u}) + \dots,$$

(1.3)

where $\overline{\boldsymbol{K}}_0$ is a second-order tensor and $\overline{f}, \overline{g}$ are bilinear and trilinear functions, respectively. The relation $V = a^2 \Delta P/\mu L$, inspired by the homogenization theory, is not universally adopted; one may pick V as a known scale and choose $\Delta P = \rho V^2$. Then, setting $\boldsymbol{u} = V\bar{u}$, using $\tilde{\nabla} p$ as the pressure gradient scaled by $\rho V^2/L$, and defining $R_e = Va/\nu$, (1.3) gives

$$-R_e \tilde{\boldsymbol{K}}_0 \cdot \tilde{\nabla} p = \bar{u} + R_e \overline{f}(\bar{u}, \bar{u}) + R_e^2 \overline{g}(\bar{u}, \bar{u}, \bar{u}) + \dots.$$

(1.4)

In dimensional form, (1.3) and (1.4) give

$$-\frac{1}{\mu} \boldsymbol{K}_0 \cdot \nabla p = \boldsymbol{u} + \frac{1}{\nu} f(\boldsymbol{u}, \boldsymbol{u}) + \frac{1}{\nu^2} g(\boldsymbol{u}, \boldsymbol{u}, \boldsymbol{u}) + \dots,$$

(1.5)

where the tensor $\boldsymbol{K}_0$ and the functions f and g are given by

$$\boldsymbol{K}_0 = a^2 \overline{\boldsymbol{K}}_0 = aL\tilde{\boldsymbol{K}}_0, \quad f = a\overline{f}, \quad g = a^2 \overline{g}.$$

(1.6)

The question of the exact form and magnitude of the nonlinear effects has been raised by Forchheimer (1901) and up to now does not seem to have received a commonly accepted answer. A review of several *ad hoc* models proposed to account for the nonlinear deviations can be found in Muskat (1946, pp. 57–69). Without "entering into an attempt to explain the possible discrepancy between" the many models, this author suggests that a possibly convenient way of looking at this problem is to represent the quantity $R_e \Delta P/\rho V^2$ as a function of the number VL/ν. This type of representation seems to have been introduced by Lindquist (1930). In this representation (cf. figure 1) Muskat distinguishes three zones. The first is called the Darcy zone, where deviations are small and Darcy's law is an acceptable model; according to Muskat (1946, p. 67), the upper limit of this zone is uncertain and depends on the choices of the scales on which the Reynolds number is built. The third zone corresponds to high-Reynolds-number flows. In this zone the nonlinear effects are dominant, and the experiments of Lindquist (1930) suggest that the deviation from Darcy's law is linear with respect to the Reynolds number (or quadratic in terms of the seepage velocity). The second zone is the transition zone between the two others. As suggested by Muskat (1946), part of the confusion raised around this problem comes from the desire of investigators to either unify the three zones into a single formula and/or to give predominance to the third zone. In this respect the experiments of Lindquist (1930) are very representative. This series of experiments have been carried out on beds of carefully calibrated lead balls. The range of Reynolds numbers that have been explored is $0 < R_e \leqslant 180$ (other authors have reached $R_e \approx 1000$); within this range, the so-called Darcy zone, extending from $0 \leqslant R_e \leqslant 4$, is of negligible extent and the quantity $R_e \Delta P/\rho V^2$ is accurately approximated by the relation $a + bR_e$ over the range $0 < R_e \leqslant 180$. This conclusion, however, omits the fact that the Reynolds numbers considered are out of the range of most practical applications, as said in Muskat (1946, p. 67), "While very high rates of flow in exceptional cases of
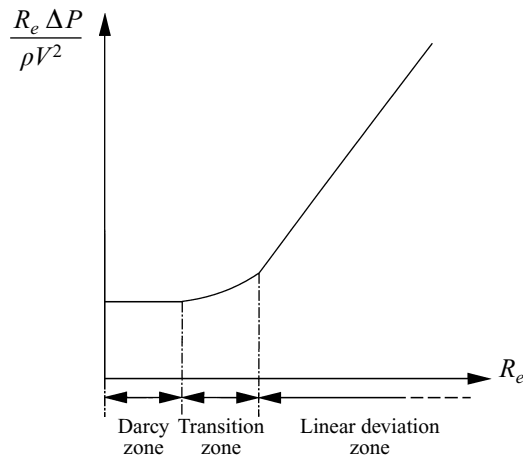
FIGURE 1. Muskat's model of flow regimes in porous media is composed of three zones.
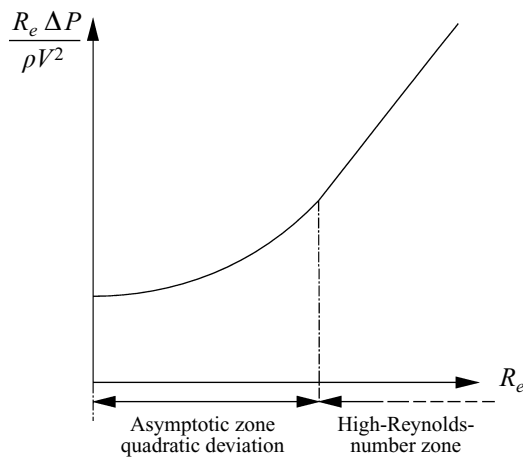

FIGURE 2. Present model of nonlinear deviations from Darcy's law: in the asymptotic zone $R_e \to 0$, the deviation is quadratic in general (one-dimensional flows or a reversibility hypothesis is satisfied).

practical flow systems will undoubtedly correspond to Reynolds numbers appreciably exceeding 1, it is unlikely that the [Reynolds number based on] macroscopic velocities in actual flow systems carrying liquids will frequently exceed that [value]". Indeed, the most frequent practical applications (for either gas or liquids) involve Reynolds numbers of order 1 or less. The purpose of this paper is to show that the Darcy zone and the transition zone emphasized by Muskat merge into one unique zone, which corresponds to the asymptotic behaviour $R_e \to 0$, and in this zone the first correction term in (1.3) is zero in general: i.e. $\overline{f} = 0$, as represented in figure 2.

The asymptotic character of this problem has been recognized recently and has led to some interesting results. For instance, it is now clear that for one-dimensional flows, the incompressibility is responsible for the vanishing of the first correction term, i.e. $\overline{f} = 0$ as $R_e \to 0$; a proof of this property can be found in §3, or in Mei & Auriault (1991) and Wodie & Levy (1991). Experiments together with numerical simulations of one-dimensional flows are reported in Rasoloarijaona & Auriault (1994). For the multi-dimensional case we refer to Mei & Auriault (1991) and

Wodie & Levy (1991), where a thorough analysis of the nonlinear corrections is made by using the two-scale asymptotic technique. It is reported in these two references that the first nonlinear correction is zero if the porous medium is isotropic; furthermore, both references give a constructive method to compute the coefficients of the second-order correction to Darcy's law.

The main objective of this paper is to show that in many cases the first correction term is zero, i.e. $\overline{f} = 0$, as the Reynolds number vanishes, and that the isotropy hypothesis, though sufficient, is not necessary to reach this conclusion. Our reasoning is threefold. First, in §2 we review a series of filtration experiments that have been performed by Darcy (1856), Hazen (1895), and Chauveteau (1965). By using proper scalings and restricting our investigation in the limit of vanishing Reynolds numbers, we discover that, for the filtration experiments we have analysed, the first nonlinear correction is zero up to the experimental errors. Second, in §3 we carry out a theoretical investigation. By assuming a reversibility hypothesis that we call (H), we prove (by the energy technique) that the first nonlinear correction is zero in unbounded periodic porous media. The hypothesis (H) means that, for a filtration experiment, if the pressure gradient is reversed, the seepage velocity should also be reversed with no change in modulus. The result of the experiment (i.e. the flow rate) may depend on the direction of the pressure gradient but not on its sign. In particular, hypothesis (H) is satisfied exactly if the microscopic cell is invariant by a reflection about one of its points. Finally, in §4 we perform numerical experiments to illustrate and test hypothesis (H). These simulations confirm our theoretical results and indicate that hypothesis (H) is satisfied in general even if the microscopic cell has no symmetry. However, for a counterexample for which (H) is not numerically satisfied, we show that the nonlinear correction is linear with respect to the Reynolds number. Hence, (H) being sufficient, seems also (numerically) to be necessary.

2. Experimental clues

In this section we give a brief historical overview of some landmark experiments and review some models that have been inferred from them. We show that some ambiguity (arbitrary choice) in the definition of the Reynolds number may have marred the interpretation of the experiments in question, and propose a normalization process of the data that is free of arbitrariness. In the light of the proposed normalization, we show that Darcy's own experiments contain a nonlinear deviation from his famous law, which is nearly quadratic in the Reynolds number. Furthermore, by applying our normalization procedure, we show that the experiments of Hazen (1895) contain a quadratic deviation to Darcy's law in the limit of vanishing Reynolds numbers in disagreement with the claim by Forchheimer (1901). Our analysis also reveals that the same quadratic deviation is present in experiments by Chauveteau (1965).

2.1. *Ambiguity in the Reynolds number and normalization*

We emphasize here, like Muskat (1946, p. 66), that there is "an inherent ambiguity in the definition of the quantities entering in the Reynolds number," which lies in the many possible choices of the macroscopic length scale, the pressure drop, and the microscopic length scale. These arbitrary choices introduce a numerical factor in the definition of the Reynolds number. From a theoretical point of view, this ambiguity is without importance since the product of any dimensionless variable and its scale remains constant, and the asymptotic analysis (i.e. $R_e \to 0$) is independent of any possible numerical factor in the Reynolds number. However, in interpreting numerical

experiments that have a limited accuracy, the ambiguity is important. For instance, assume that we want to test the following one-dimensional nonlinear filtration law:

$$-\frac{1}{\mu}\boldsymbol{K}_0 \cdot \nabla p = \boldsymbol{u} + \bar{\alpha}\frac{a}{v}|\boldsymbol{u}|^2 + \bar{\beta}\frac{a^2}{v^2}|\boldsymbol{u}|^2\boldsymbol{u} + \dots$$

and that we can choose between two definitions of the Reynolds number, say R_e and R'_e. Let us for each case denote by $(\bar{\alpha}, \bar{\beta})$ and $(\bar{\alpha}', \bar{\beta}')$ the coefficients of the nonlinear effects in the relation above. They are linked by the relations

$$\frac{\bar{\alpha}}{\bar{\alpha}'} = \frac{R'_e}{R_e}, \quad \frac{\bar{\beta}}{\bar{\beta}'} = \frac{R'^2_e}{R^2_e}.$$

One measure of the relative importance of the first- and second-order correction terms is the ratio $\bar{\alpha}/\bar{\beta}$, which depends on the definition of the Reynolds number, since

$$\frac{\bar{\alpha}'}{\bar{\beta}'} = \frac{\bar{\alpha}}{\bar{\beta}}\frac{R'_e}{R_e}.$$

Assume, for instance, that R_e/R'_e is equal to $1/10$; if in the first case $\bar{\alpha} = \bar{\beta}$, the linear and bilinear corrections are of the same order, whereas in the second case (with exactly the same experimental data) the linear correction is ten times the bilinear one. Of course, the risks of misinterpretations are increased if instead of using dimensionless quantities one uses physical data (i.e. dimension dependent) as was done by Forchheimer (1901).

In order to avoid this ambiguity, we propose the following normalization procedure. Since we are interested in measuring the relative effects of some phenomenon on some range of Reynolds number, say $0 \leqslant R_e \leqslant R_{e,max}$, we choose $R_{e,max}$ as a new reference by introducing the new variable

$$x = \frac{R_e}{R_{e,max}}. \tag{2.1}$$

Furthermore, since we are interested in the deviation from Darcy's law, we should consider the magnitude of $(\boldsymbol{u} + \boldsymbol{K}_0 \cdot \nabla p)/|\boldsymbol{u}|$. In order to compare only dimensionless numbers, we introduce the variable $y = (y_1, \dots, y_n)$, where n is the space dimension ($n = 2$ or 3):

$$y_i = \frac{1 + (\boldsymbol{K}_0 \cdot \nabla p)_i/\mu u_i}{1 + (\boldsymbol{K}_0 \cdot \nabla p_{i,max})/\mu u_{i,max}}, \tag{2.2}$$

where the subscript *max* refers to the value measured at $R_{e,max}$. With this new definition we have

$$y_i = a_i x + b_i x^2 + c_i x^3 + \dots$$

with $a_i + b_i + c_i + \dots = 1$. Of course, this rescaling makes sense only if the deviation is experimentally significant. If the experimental data are on the line $y = x$, it means that the deviation is linear, whereas if the data collapse on the parabola $y = x^2$, the deviation is quadratic and the contribution of the linear term is zero. The nonlinear deviation will be zero within some range of Reynolds numbers if the data are on the line $y = 0$.

2.2. *Darcy's experiment*

In this subsection we reinterpret Darcy's experiments in the light of the renormalization process introduced above. Darcy's experiments were carried out on a column

Experiment number	Duration (min)	Average flow rate ($l \min^{-1}$)	Pressure drop (m of H_2O)	Ratio between flow rate and pressure drop	Comments
1	25	3.60	1.11	3.25	Sand was not washed
2	20	7.65	2.36	3.24	
3	15	12.00	4.00	3.00	
4	18	14.28	4.90	2.91	Only small oscillations
5	17	15.20	5.02	3.03	in the pressure column
6	17	21.80	7.63	2.86	
7	11	23.41	8.13	2.88	Sizable oscillations
8	15	24.50	8.58	2.85	
9	13	27.80	9.86	2.82	Strong oscillations
10	10	29.40	10.89	2.70	

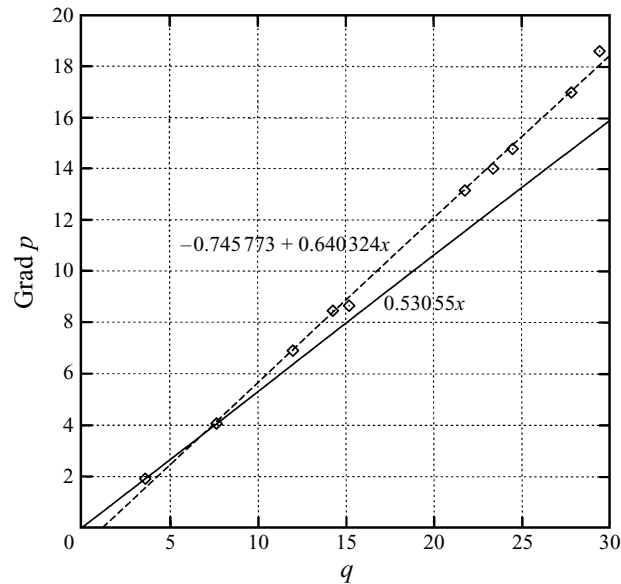TABLE 1. Data from Darcy's experiment

FIGURE 3. Pressure gradient versus flow rate for Darcy's experiment. Experimental data (symbols), linear least-square fit (dashed line), physically coherent Darcy model (solid line).

with diameter and height 0.35 m and 3.5 m, respectively. Darcy also reported five experiments in his book; three heights of sand bed have been tested: 0.58 m, 1.14 m, and 1.70 m. The most complete experiment is that with the 0.58 m sand bed. His data are collected in table 1. In figure 3, the pressure gradient (i.e. ratio of the pressure drop to the bed height) is plotted as a function of the flow rate (symbols); the dashed line is a linear fit of the experimental data by the least-square approximation $-\nabla p = -0.745773 + 0.640324q$. Note that this fit yields a negative pressure gradient when the flow rate is zero; hence, besides possible experimental errors, the linear fit may not be satisfactory. In order to build a physically acceptable fit that passes through the origin, we assume that Darcy's law is valid in the range of vanishing flow rates. The solid line in figure 3 represents Darcy's law obtained under this hy-
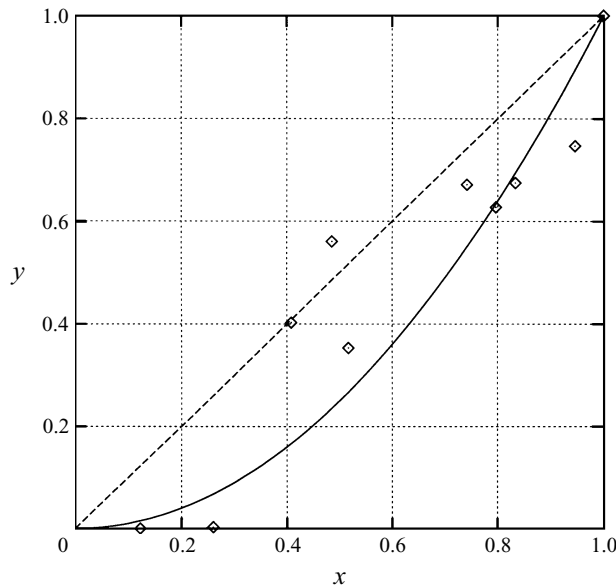
FIGURE 4. Deviation of Darcy's data from Darcy's law. Experimental data (symbols), linear deviation (dashed line), quadratic deviation (solid line).

pothesis; it passes through the origin and the first two data points. We see that as the flow rate increases, the experimental data tend to deviate from the linear relation, implying a deviation from Darcy's law. Actually, though Darcy recognized in a first approximation a linear relation between the flow rate and the pressure drop, he was also well aware of deviations and tried to ascribe their origin to some experimental flaws (Darcy 1856, pp. 592–593).

In order to illustrate the normalization process described in the subsection above, we apply it to Darcy's experiments. In figure 4, the normalized deviation (difference between the data and the solid line in figure 3) is plotted. In this figure, Darcy's law only applies to the first point (indeed, we made it an assumption) and the second point. As a whole, the experiments show a coherent deviation from Darcy's law. If we dismiss data points 3 and 4, which may be plagued by experimental errors, the deviation is well represented by the parabola x^2, which in turn would suggest a quadratic deviation from Darcy's law. However, there are not enough data to test the coherence of points 3 and 4; one can only conclude that Darcy's own experiments contained some nonlinear deviation from his law.

2.3. *Forchheimer's analysis*

In two articles on the nonlinear deviations from Darcy's law, Forchheimer (1901) proposes three *ad hoc* formulae:

$$\alpha = av + bv^2, \quad \alpha = mv^n, \quad \text{and} \quad \alpha = av + bv^2 + cv^3,$$

where α is the ratio of the pressure drop (measured in height of water) to the thickness of the sand bed and v is the seepage velocity (measured in metres per day). Here, we emphasize that although Forchheimer's analysis may be of some engineering value, no physical conclusion can reasonably be drawn from it by comparing the relative value of coefficients a, b, and c, for it uses the dimensional quantity v. This problem has far

		Experiment number		
	III	IV	V	VI
		Sand diameter (mm)		
	0.75	0.90	0.90	1.35
$\alpha \times 10^2$		Seepage velocity (m/day)		
0.05	20	30	50	80
0.10	41	58	100	148
0.20	78	110	190	275
0.40	150	208	350	480
0.60	207	275	450	620
0.80	252	340	530	720
1.0	300	385	610	830
1.5	378	480	760	1030
2.0	467	580	890	1180
3.0	615	750	1110	1450
5.0	885	1060	1490	
10.0	1310	1550		

TABLE 2. Hazen's data

more consequences than the ambiguity in the definition of the Reynolds number we have addressed above.

Forchheimer has analysed the data from experiments performed by other authors such as Hazen (1895). In order to illustrate that Forchheimer's analysis may have been blurred by not using proper dimensionless variables and not working in the asymptotic range $R_e \to 0$, we hereafter apply our normalization procedure to four experiments of Hazen and show that, in the range of vanishing Reynolds numbers, the deviation from Darcy's law is indeed quadratic (in the dimensionless form (1.3)). Hereafter we concentrate on Hazen's experiments, referred to by Forchheimer as III, IV, V, and VI, which correspond to filtration experiments on consolidated sand beds with sand grains of mean diameter 0.75, 0.90, 0.90 and 1.35 mm, respectively. The data are reported in table 2. For each experiment, the approximate maximum Reynolds number reported is 9.0, 13.5, 12.9, and 18.9, respectively. The normalized representation of these data is plotted in figure 5; for each experiment we have chosen, respectively, $R_{e,max} = 2.6, 4.2, 6.6$, and 15.4 (in m/day the corresponding velocities are 378, 480, 760, and 1180). Allowing for possible experimental errors, this plot clearly shows that the deviation is quadratic and not linear, contrary to what Forchheimer inferred from these data.

2.4. *Chauveteau's experiments*

We end our review of experimental data by including five experiments by Chauveteau (1965). Contrary to the natural sand experiments referred to above, Chauveteau used re-constructed periodic porous media.

The first experiment concerns the flow in a two-dimensional canal with sawtooth walls, the saw pattern being symmetric with respect to the direction orthogonal to the canal's axis (model E). As a consequence of the symmetry condition, the flow is reversible. The second and third experiments were carried out in a canal with non-symmetric sawtooth walls; consequently, inertia effects tend to break the symmetry of the flow. Depending on the direction of the flow the experiment is referred to as G_1 or G_2. The fourth experiment was performed in a two-dimensional canal with parallel walls of sinusoidal profile; this is referred to as experiment H. The last
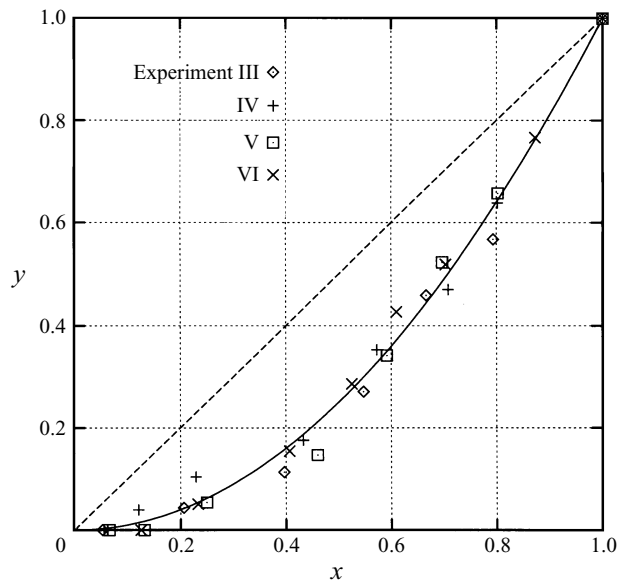
FIGURE 5. Deviation of Hazen's data from Darcy's law. Experimental data (symbols), linear deviation (dashed line), quadratic deviation (solid line).

Model E		Model G$_1$		Model G$_2$		Model H		Model I	
R_e	$R_e\nabla p$	R_e	$R_e\nabla p$	R_e	$R_e\nabla p$	R_e	$R_e\nabla p$	R_e	$R_e\nabla p$
6.96	29.65	7.39	32.22	6.01	32.03	13.2	45.70	1.11	22.70
10.1	29.69	16.4	32.26	19.8	32.20	22.0	45.88	2.46	22.75
16.9	29.91	29.1	32.80	32.1	32.61	27.6	45.82	3.94	23.00
26.6	29.98	40.8	33.49	43.7	33.25	32.1	45.74	6.21	23.28
31.5	30.24	65.6	34.44	57.5	33.35	43.4	45.22	8.82	23.72
37.8	30.77	68.3	51.70	81.5	34.63	54.2	46.68	11.2	24.64
46.6	31.78	84.2	36.95			62.0	47.37		
55.9	32.30					79.1	50.62		
						108.0	55.07		
						146.0	64.39		
						194.0	77.99		

TABLE 3. Chauveteau's data

experiment attempts to simulate two-dimensional flows in a real porous media. For this purpose, Chauveteau constructed a two-dimensional model 200 mm long, 32 mm wide, and 7 mm thick, and randomly placed cylinders resembling sand grains in cross-section. This model is referred to as model I. Note, however, that the interpretation of this experiment is ambiguous in the limit $R_e \to 0$, for unless the permeability tensor of the model is isotropic or the direction of the measurement coincides with one principal axis of the permeability tensor, the lateral confinement of the flow dramatically affects the measurement. Since no verification of the two hypotheses mentioned above is reported in Chauveteau (1965), it is likely that this experiment is actually one-dimensional.

The data corresponding to small values of the Reynolds number for experiments E, G$_1$, G$_2$, H, and I are reported in table 3. The normalized representation of these
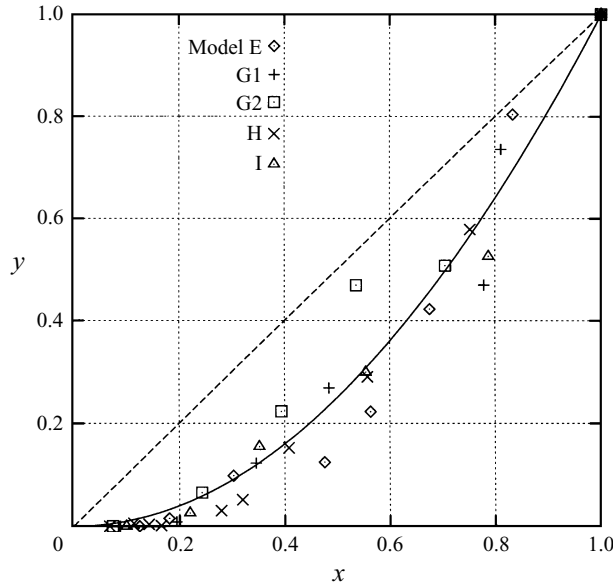
FIGURE 6. Normalized representation of the deviation from Darcy's law for Chauveteau's experiments, Experimental data (symbols), linear deviation (dashed line), quadratic deviation (solid line).

data is shown in figure 6, which illustrates once more that in the range of vanishing Reynolds numbers the deviation from Darcy's law (in the dimensionless form (1.3) or (1.4)) is quadratic in the Reynolds number.

We have shown is this section that by adopting a normalized representation of nonlinear effects, it is possible to reinterpret well-known filtration experiments. In particular, besides possible experimental errors, Darcy's experiments contain some deviation from the linear filtration law. We have analysed Hazen's experiments which Forchheimer used to support his theories, and clearly showed that in the limit of vanishing Reynolds number, the nonlinear effects are quadratic (cf. figure 5). This is further supported by Chauveteau's filtration experiments (cf. figure 6). In the next section, we show that these experimental observations can be theoretically confirmed if the porous medium is periodic.

3. A theoretical result for periodic media

For unbounded periodic porous media, we prove that the first correction term to Darcy's law is zero provided a reversibility hypothesis (H) is satisfied.

3.1. *Definitions and preliminaries*

Consider Ω a parallelepipedic periodic cell in $\mathbb{R}^n$ the sides of which are the vectors $(t_1, \dots, t_n)$ assumed to be independent (see figure 7). For $i = 1, \dots n$ we denote by $\Gamma_i^{\pm}$ the faces of Ω so that $\Gamma_i^+ = \Gamma_i^- + t_i$. Let Ω_0 be an open connected subdomain of Ω. The boundary of Ω_0, denoted by Γ_0, is assumed to be smooth. The subdomain Ω_0 is filled with an incompressible viscous fluid, whereas its complement in Ω is solid. For $i = 1, \dots, n$ we set $\Gamma_{i,p}^{\pm} = \Gamma_i^{\pm} \cap \Gamma_0$, and we assume that Ω_0 is compatible with the periodicity in the sense that $\Gamma_{i,p}^+ = \Gamma_{i,p}^- + t_i$ ($\Gamma_{i,p}^-$ and $\Gamma_{i,p}^+$ are the two periodic boundaries of the fluid domain in the direction t_i). We also define $\Gamma_{0,s} = \Gamma_0 \setminus \cup_{i=1}^n \Gamma_{i,p}^{\pm}$.
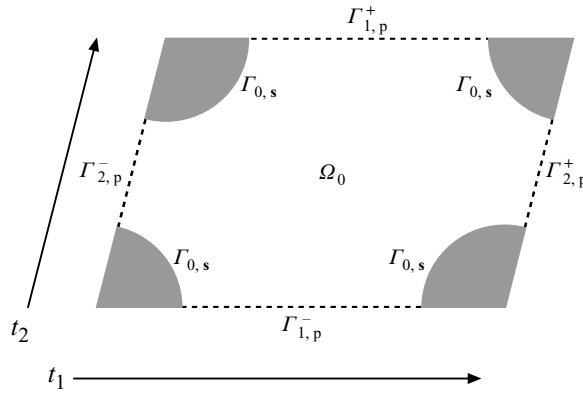
FIGURE 7. Definition of the periodic cell and notation.

We assume that $\mathrm{meas}(\Gamma_{0,s}) \neq 0$ and $\mathrm{meas}(\Gamma_{i,p}^-) \neq 0$ for $i = 1,\ldots,n$ ($\Gamma_{0,s}$ is the fluid boundary that is in contact with the solid).

Now we consider the creeping flow that is induced in Ω_0 by an external pressure gradient $-\lambda$ with $|\lambda| = 1$ (i.e. the scale of the macroscopic pressure gradient is given). We assume periodic boundary conditions on $\Gamma_{i,p}^\pm$ and no-slip boundary conditions on $\Gamma_{0,s}$ (i.e. the solid). In order to work within a variational framework, we introduce the usual Sobolev space $\mathrm{H}_{0,p}^1(\Omega_0) = \{\boldsymbol{v} \in \mathrm{H}^1(\Omega_0),\ \boldsymbol{v}_{|\Gamma_{0,s}} = 0,\ \boldsymbol{v}_{|\Gamma_{i,p}^-} = \boldsymbol{v}_{|\Gamma_{i,p}^+}\}$ together with $V = \{\boldsymbol{v} \in \mathrm{H}_{0,p}^1(\Omega_0),\ \mathrm{div}\,\boldsymbol{v} = 0\}$, which is composed of the divergence-free vector fields of $\mathrm{H}_{0,p}^1(\Omega_0)$.

We denote by $\boldsymbol{u}_0(\lambda)$ the velocity field induced by the pressure gradient $-\lambda$ in Ω_0. Then, one can show that there is a periodic pressure field $p_0(\lambda)$ so that $(u_0(\lambda), p_0(\lambda))$ is the solution to the following boundary value problem:

$$\left.\begin{array}{l} -\nabla^2\boldsymbol{u}_0(\lambda) + \nabla p_0(\lambda) = \lambda, \\ \nabla \cdot \boldsymbol{u}_0(\lambda) = 0, \\ \boldsymbol{u}_{0|\Gamma_{0,s}}(\lambda) = 0, \\ \boldsymbol{u}_{0|\Gamma_{i,p}^-}(\lambda) = \boldsymbol{u}_{0|\Gamma_{i,p}^+}(\lambda), \quad p_{0|\Gamma_{i,p}^-}(\lambda) = p_{0|\Gamma_{i,p}^+}(\lambda). \end{array}\right\} \tag{3.1}$$

Note that, within the two-scale asymptotic framework developed in Mei & Auriault (1991) and Wodie & Levy (1991), $\boldsymbol{u}_0(\lambda)$ is the first term of the asymptotic expansion of the velocity with respect to the small parameter measuring the ratio of the pore size of the porous structure to the macroscopic length scale at hand. Within a variational framework, this velocity is the solution to the following variational Stokes problem:

$$\forall \boldsymbol{v} \in \boldsymbol{v}, \quad (\nabla \boldsymbol{u}_0(\lambda), \nabla \boldsymbol{v}) = (\lambda, \boldsymbol{v}). \tag{3.2}$$

Given the hypotheses on Ω_0, this problem is well posed and enables us to introduce the permeability tensor $\boldsymbol{K}_0 \in \mathscr{L}(\mathbb{R}^n, \mathbb{R}^n)$ so that

$$\boldsymbol{K}_0\lambda = \frac{1}{\mathrm{meas}(\Omega_0)} \int_{\Omega_0} \boldsymbol{u}_0(\lambda). \tag{3.3}$$

The first important result concerning this tensor is that

LEMMA 1. $\boldsymbol{K}_0$ *is symmetric and positive definite.*

In the framework of the homogenization theory, the relation $\boldsymbol{K}_0\lambda = \int_{\Omega_0} \boldsymbol{u}_0(\lambda)/$ meas(Ω_0) is interpreted as Darcy's law (cf. Allaire 1989, Bensoussan, Lions & Papanicloaou 1978; Sanchez-Palencia 1980; Tartar 1980). The goal of this section is to give a bound on the nonlinear correction to this relation for small inertia effects.

3.2. *Nonlinear deviation in two and three dimensions*

Assume now that the dimension is $n = 2$ or 3. Let $\Delta P/L$ be a characteristic scale of the macroscopic pressure gradient to be applied on the porous medium, then we define the microscopic Reynolds number, δ, as follows:

$$\delta = \frac{\rho \Delta P a^3}{L \mu^2}, \tag{3.4}$$

where ρ is the fluid density, a is the characteristic microscopic length scale, and μ is the dynamic viscosity of the fluid. It results from these choices that the velocity scale is necessarily equal to $\Delta P a^2/\mu L$. Let ϵ be the ratio of the microscopic length scale to the macroscopic one, $\epsilon = a/L$; then, we have $\delta = \rho \Delta P L^2 \mu^{-2} \epsilon^3$. To avoid the technical difficulties of having to consider the limit for two small parameters $\epsilon \to 0$ and $\delta \to 0$, it is convenient within the two-scale homogenization theory to assume that $\rho \Delta P L^2 \mu^{-2}$ is equal to $c_0 \epsilon^{-2\beta}$ for some β, where c_0 is a numeric constant of order unity. As a result, the microscopic Reynolds number is assumed to be of the form $c_0 \epsilon^{3-2\beta}$. Since we are interested in the limit $\delta \to 0$, we assume that $\beta \leqslant 3/2$ (we shall recover the Darcy limit when $\epsilon \to 0$); furthermore, we assume that $1 \leqslant \beta$ so that the terms of $O(\delta)$ are larger than the local corrections of $O(\epsilon)$ induced by the presence of the pores. Hence, the theory that follows should be of practical use under the following hypothesis: there is some β such that

$$1 \leqslant \beta \leqslant 3/2, \text{ and } \frac{v}{(\Delta P/\rho)^{1/2}L} = c_1 \epsilon^\beta. \tag{3.5}$$

The condition $\beta \leqslant 3/2$ yields an upper bound on the macroscopic Reynolds number $((\Delta P/\rho)^{1/2}L/v)$ for which the asymptotic analysis is valid, whereas the condition $1 \leqslant \beta$ requires the macroscopic Reynolds number to be high enough so that the nonlinear effects can be seen.

We are now interested in solving the following variational Navier–Stokes problem: for $\delta \geqslant 0$ and $\lambda \in S_n(0,1)$, find $u_\delta(\lambda) \in V$ such that

$$\forall \boldsymbol{v} \in V, \quad (\nabla \boldsymbol{u}_\delta(\lambda), \nabla \boldsymbol{v}) + \delta(\boldsymbol{u}_\delta(\lambda) \cdot \nabla \boldsymbol{u}_\delta(\lambda), \boldsymbol{v}) = (\lambda, \boldsymbol{v}). \tag{3.6}$$

This problem is well posed thanks to the Poincaré inequality and a general existence theorem based on Brouwer's fixed point theorem (e.g. cf. Girault & Raviart 1986, theo. 1.3, p. 282). The solution is unique if $\delta < c_p(\Omega_0)^2/2c_b\text{meas}(\Omega_0)$, where $c_p(\Omega_0)$ is the Poincaré constant of the domain Ω_0 and c_b is the norm of the skew-symmetric trilinear form $(\boldsymbol{u} \cdot \nabla \boldsymbol{v}, w)$ on $H^1_{0,p}(\Omega_0)^3$. It can be shown that there is a periodic pressure field $p_\delta(\lambda)$ such that $(\boldsymbol{u}_\delta(\lambda), p_\delta(\lambda))$ is formally the solution to the following Navier–Stokes problem:

$$\left. \begin{array}{l} -\nabla^2 \boldsymbol{u}_\delta(\lambda) + \delta \boldsymbol{u}_\delta(\lambda) \cdot \nabla \boldsymbol{u}_\delta(\lambda) + \nabla p_\delta(\lambda) = \lambda, \\ \nabla \cdot \boldsymbol{u}_\delta(\lambda) = 0, \quad \boldsymbol{u}_{\delta|\Gamma_{0,s}}(\lambda) = 0, \\ \boldsymbol{u}_{\delta|\Gamma_{i,p}^-}(\lambda) = \boldsymbol{u}_{\delta|\Gamma_{i,p}^+}(\lambda), \quad p_{\delta|\Gamma_{i,p}^-}(\lambda) = p_{\delta|\Gamma_{i,p}^+}(\lambda). \end{array} \right\} \tag{3.7}$$

We now seek a relation between $\int_{\Omega_0} \boldsymbol{u}_\delta(\lambda)$ and λ when δ is small. For this purpose we introduce an expansion for $\boldsymbol{u}_\delta$ as follows: $\boldsymbol{u}_\delta = \boldsymbol{u}_0 + \delta\boldsymbol{u}_1 + \ldots$. More precisely (and rigorously), we define $\boldsymbol{u}_0(\lambda) \in V$ and $\boldsymbol{u}_1(\lambda) \in V$ so that

$$\forall v \in \boldsymbol{u}, \quad (\nabla\boldsymbol{u}_0(\lambda), \nabla v) = (\lambda, v), \tag{3.8}$$

and

$$\forall v \in V, \quad (\nabla\boldsymbol{u}_1(\lambda), \nabla v) = -(\boldsymbol{u}_0(\lambda) \cdot \nabla\boldsymbol{u}_0(\lambda), v). \tag{3.9}$$

THEOREM 3.1. *If δ is small enough (namely, if $\delta < c_p(\Omega_0)^2/2c_b\mathrm{meas}(\Omega_0)$), we have the following bounds:*

$$|\boldsymbol{u}_\delta(\lambda) - \boldsymbol{u}_0(\lambda)|_1 \leqslant \delta c_b/c_p(\Omega_0)^3, \tag{3.10}$$

$$|\boldsymbol{u}_\delta(\lambda) - \boldsymbol{u}_0(\lambda) - \delta\boldsymbol{u}_1(\lambda)|_1 \leqslant 2\delta^2 c_b^2/c_p(\Omega_0)^4. \tag{3.11}$$

That is to say, $\boldsymbol{u}_0(\lambda) + \delta\boldsymbol{u}_1(\lambda)$ is a good approximation of $\boldsymbol{u}_\delta(\lambda)$ in $\mathrm{H}_{0,p}^1(\Omega_0)$; in other words, δ induces a regular perturbation to the Stokes flow. Hence, it is reasonable to seek a relation between $\int_{\Omega_0} \boldsymbol{u}_\delta(\lambda)$ and λ in the form of a perturbation of Darcy's law.

We now introduce the main hypothesis of this work:

(H) *For all $\lambda \in S_n(0, 1)$ (the sphere in $\mathbb{R}^n$) and δ small enough, we assume that $u_\delta(\lambda)$ satisfies*

$$\int_{\Omega_0} \boldsymbol{u}_\delta(\lambda) = -\int_{\Omega_0} \boldsymbol{u}_\delta(-\lambda) + O(\delta^2). \tag{3.12}$$

This hypothesis means that if the pressure gradient is reversed, the seepage velocity should also be reversed up to a perturbation term of $O(\delta^2)$. The experimental flow rate $\int_{\Omega_0} \boldsymbol{u}_\delta$ may depend on the direction of the pressure gradient. This hypothesis is physically reasonable and is compatible with certain types of anisotropy as explained below.

The main result of this section is that

THEOREM 3.2. *If hypothesis (H) is satisfied, we have*

$$\forall \lambda \in S_n(0, 1), \quad \frac{1}{meas(\Omega_0)} \int_{\Omega_0} \boldsymbol{u}_\delta(\lambda) = \boldsymbol{K}_0\lambda + O(\delta^2). \tag{3.13}$$

Proof. In view of the bound (3.11), we have

$$\int_{\Omega_0} \boldsymbol{u}_\delta(\lambda) = \int_{\Omega_0} \boldsymbol{u}_0(\lambda) + \delta\int_{\Omega_0} \boldsymbol{u}_1(\lambda) + O(\delta^2).$$

Furthermore, hypothesis (H) implies that

$$\int_{\Omega_0} \boldsymbol{u}_0(-\lambda) + \delta\int_{\Omega_0} \boldsymbol{u}_1(-\lambda) = -\int_{\Omega_0} \boldsymbol{u}_0(\lambda) - \delta\int_{\Omega_0} \boldsymbol{u}_1(\lambda) + O(\delta^2).$$

Since the dependence of u_0 on λ is linear and that of u_1 is quadratic, we infer that $\int_{\Omega_0} \boldsymbol{u}_1(\lambda) = 0$. As a result we have

$$\int_{\Omega_0} \boldsymbol{u}_\delta(\lambda) = \int_{\Omega_0} \boldsymbol{u}_0(\lambda) + O(\delta^2),$$

which yields the desired result, for by definition $\int_{\Omega_0} \boldsymbol{u}_0(\lambda) = \mathrm{meas}(\Omega_0)\boldsymbol{K}_0\lambda$. $\square$

The result (3.13) means that if δ is small enough, the seepage velocity almost satisfies Darcy's law with the permeability tensor $\boldsymbol{K}_0$; the norm of the nonlinear correction is bounded from above by $c\delta^2$, where the constant c depends only on the geometry of the domain.

In Mei & Auriault (1991) and Wodie & Levy (1991), a similar result is proved provided the porous medium is assumed to be isotropic. The main result of the present paper is that the macroscopic isotropy hypothesis, though sufficient, may be weakened and extended by the microscopic hypothesis (H). This hypothesis can be further characterized as follows:

We shall say that Ω_0 is invariant by central symmetry if there are n planes (not necessarily orthogonal) such that Ω_0 is symmetrical with respect to these n planes (n is the space dimension). If Ω_0 is invariant by central symmetry, then (H) is satisfied and the $O(\delta^2)$ term is exactly zero. This is because the Navier–Stokes equations are invariant by reflection. The cell represented in figure 8(*b*) satisfies this hypothesis.

If Ω_0 is invariant under the transformation S_i, $i = 1, \ldots, n$, so that $S_i(t_i) = t_i$ and $S_i(t_j) = -t_j$ if $j \neq i$, then Ω_0 is invariant by central symmetry and (H) is satisfied.

In two dimensions, hypothesis (H) can be weakened. We may assume that there exist only two independent reversibility directions. In three dimensions, we may assume that there are four reversibility directions that are 3 by 3 linearly independent. The cell shown in figure 9(*b*) does not have the symmetry property described above; however, it can be verified numerically that the flow is reversible with respect to the *x*-direction, while the reversibility in the *y*-direction is obvious. Hence, (H) is satisfied for the cell in question (at least numerically).

If the porous medium is isotropic, then the reversibility hypothesis is trivially satisfied; however, the isotropy hypothesis is not necessary. In particular, the isotropy argument does not apply to the highly anisotropic porous structure depicted in figure 8(*b*), whereas hypothesis (H) is satisfied (given the symmetry argument); consequently, the nonlinear correction to the Darcy law in the anisotropic porous medium in question is quadratic in the Reynolds number.

Though hypothesis (H) is of a microscopic nature, it has the following macroscopic interpretation which can be exploited experimentally. For instance, let us take a raw soil sample and carry out (multi-dimensional) filtration experiments on it by applying a pressure gradient. To possibly consider anisotropic porous media, let us choose the principal axes of the porous medium as our coordinate system. Let us fix the modulus of the pressure gradient, apply this pressure gradient to the soil sample and explore all the possible orientations of the pressure gradient with respect to the principal axes of the porous medium. Assume that for each orientation we do the following: apply the pressure gradient, measure the vector flow rate, then reverse the pressure gradient and measure the corresponding vector flow rate. If for each possible orientation of the pressure gradient with respect to the principal axes of the soil sample the vector flow rates of the two experiments are equal and opposite, then hypothesis (H) is satisfied experimentally; as a result, the nonlinear deviation from Darcy's law should be cubic in terms of seepage velocity. In fact, the reversibility hypothesis is intuitively natural, since the result of filtration experiments should, in general, depend on the angle between the pressure gradient and the principal axes of the sample, whereas it should not depend on the sign of the pressure gradient. In other words, since in general the results of the experiments should not change when the sample is turned upside down in the experimental set-up that enforces the pressure gradient, the nonlinear deviation should be cubic with respect to the seepage velocity in general, provided the limiting condition (3.5) is satisfied.

3.3. *Nonlinear deviation for one-dimensional flows*

An equivalent result can be proved for one-dimensional flows without any other hypothesis than the incompressibility of the flow as already shown in Wodie & Levy (1991), Mei & Auriault (1991), and Bourgeat & Marušić-Paloka (1995). We include this result here for the sake of completeness. More precisely, we assume now that $\text{meas}(\Gamma_{i,p}^-) = 0$ for $i = 2, \ldots, n$. Let $(t^1, \ldots, t^n)$ be the contravariant basis associated with $(t_1, \ldots, t_n)$, then it is an easy matter of calculus to show the identity

$$i = 1, \ldots, n, \ \forall v \in V, \quad \int_{\Omega_0} v \cdot t^i = -\int_{\Gamma_{i,p}^-} v \cdot n . \tag{3.14}$$

As a result, for all v in V we have

$$(v, t^i) = 0 \quad \text{for } i = 2, \ldots, n.$$

Noting that $\text{span}\langle t_1 \rangle = \text{span}\langle t^2, \ldots, t^n \rangle^\perp$, we infer that incompressible flows in Ω_0 are uni-dimensional in the mean and are parallel to t_1. Since the identity above is true for all $K_0 \lambda$, the range of K_0 is $\text{span}\langle t_1 \rangle$. Furthermore, since K_0 is self-adjoint, we deduce

$$\text{N}(K_0)^\perp = \text{R}(K_0) = \langle t_1 \rangle.$$

Hence, in the mean, only direction t_1 is of interest.

THEOREM 3.3. *Under the hypothesis stated above we have the following one-dimensional Darcy's law:*

$$\forall \lambda \in \{ t_1/|t_1|, -t_1/|t_1| \}, \quad \int_{\Omega_0} u_\delta(\lambda) = K_0 \lambda + O(\delta^2). \tag{3.15}$$

Proof. In order to prove this result, we first note that since $u_1(\lambda)$ is in V (*i.e.*, it is an incompressible flow), $\int_{\Omega_0} u_1(\lambda)$ is necessarily parallel to t_1 (as shown above). Furthermore, due to the (variational) definition of $u_0(\lambda)$ and $u_1(\lambda)$, it can be shown by partial integration that

$$\begin{aligned}
(u_1(\lambda), \lambda) &= (\nabla u_0(\lambda), \nabla u_1(\lambda)), \\
&= -(u_0(\lambda) \cdot \nabla u_0(\lambda), u_0(\lambda)), \\
&= +(u_0(\lambda) \cdot \nabla u_0(\lambda), u_0(\lambda)), \\
&= 0.
\end{aligned}$$

That is to say $\int_{\Omega_0} u_1(\lambda)$ is orthogonal to t_1. As a result $\int_{\Omega_0} u_1(\lambda)$ is zero, which proves the desired result, for the perturbation result (3.11) still holds. $\qquad\square$

4. Numerical simulations

4.1. *Numerical method*

In order to test the theoretical results obtained in the section above, we have performed numerical simulations on two-dimensional periodic porous media.

The computational domain is a periodic rectangular cell: $\Omega =]0, t_1[\times]0, t_2[$. The fluid domain is denoted by Ω_0, and the solid part is denoted by Ω_s. In order to take advantage of solution methods based on structured rectangular grids, we consider the fluid and the solid as a single continuous medium that satisfies the following
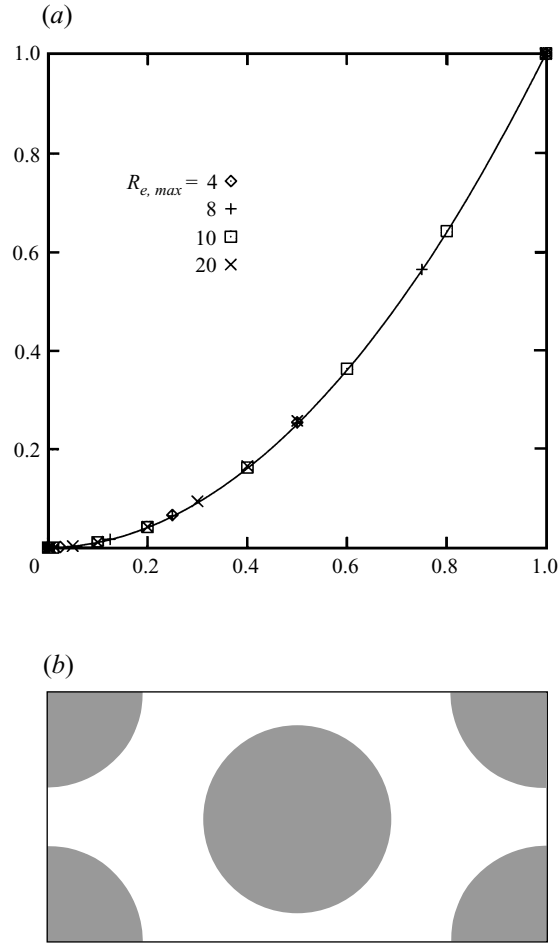
(*a*)

(*b*)

FIGURE 8. (*a*) Anisotropic case with central symmetry (see definition in text). The curve is quadratic. (*b*) Geometry of the periodic cell.

conservation equations:

$$\left.\begin{array}{l} -\nabla^2\boldsymbol{v} + \nabla p + R_e\boldsymbol{v}\cdot\nabla\boldsymbol{v} + (1/D_a)\boldsymbol{v} = \lambda, \\ \mathrm{div}\boldsymbol{v} = 0, \\ \boldsymbol{v},\ p,\ \text{periodic in } \Omega, \end{array}\right\} \tag{4.1}$$

where D_a is a penalty coefficient (something like a 'Darcy constant') that satisfies

$$D_a = 10^{30} \text{ in } \Omega_0, \quad D_a = 10^{-7} \text{ in } \Omega_s. \tag{4.2}$$

This penalization technique has been introduced by Arquis & Caltagirone (1984) and Beckermann, Ramadhyani & Viskanta (1987); it is more or less similar to the fictitious domain methods. The source term λ is a unit vector in $\mathbb{R}^2$ corresponding to the macroscopic pressure gradient with the scale $\Delta P/L$. The reference length scale is the period, a, in the x-direction of the porous medium. The velocity is scaled by $\Delta P a^2/L\mu$; as a consequence, the Reynolds number is defined by (1.2)

The numerical solution of (4.1) is obtained by a MAC approximation based on a Cartesian mesh as introduced by Harlow & Welsh (1965). The incompressibility
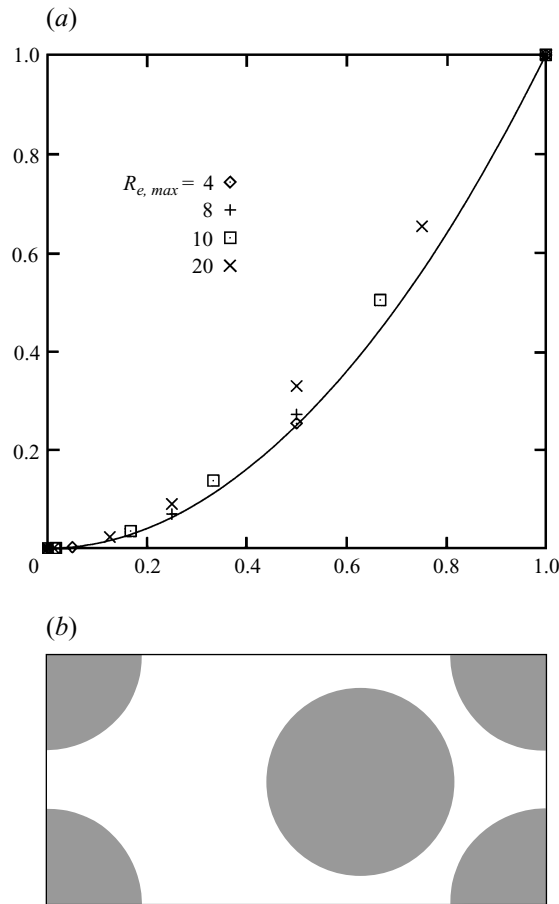
(*a*)

(*b*)

FIGURE 9. (*a*) Anisotropic case without central symmetry. The curve is quadratic. (*b*) Geometry of the periodic cell.

constraint is taken care of by means of a pseudo-time stepping and a fractional step projection method. The momentum and mass conservation equations are solved, respectively, by means of an ADI technique and a multigrid algorithm. A thorough convergence analysis of the numerical scheme has been carried out. For each configuration of the microscopic cell, the mesh has been refined until no significant variation in the results are observed. Typically, we have used meshes with about 128×128 nodes.

4.2. *Numerical results*

In the first numerical test, we consider a rectangular cell for which $|t_1|/|t_2| = 2$. The solid part is composed of cylinders as shown in figure 8(*b*). The tensor $\mathbf{K}_0$ is not isotropic; hence, the homogenized medium is not 'isotropic' with respect to the Stokes equations. The cell is reflection symmetric about the *x*- and *y*-axes; hence, (H) is satisfied. We have solved numerically the steady Navier–Stokes equations in this cell for a series of Reynolds numbers and fixed pressure gradients λ.

In figure 8(*a*) we plot the quantity $| \int_{\Omega_0} \boldsymbol{u}_\delta(\lambda) - \boldsymbol{K}_0\lambda|$ normalized by its maximum as a function of the relative Reynolds number $R_e/R_{e,max}$ for different values of $R_{e,max} \leqslant 20$ and $\lambda = \mathrm{e}^{\mathrm{i}\pi/4}$. It is evident that the nonlinear correction is quadratic for $R_e \leqslant 20$.
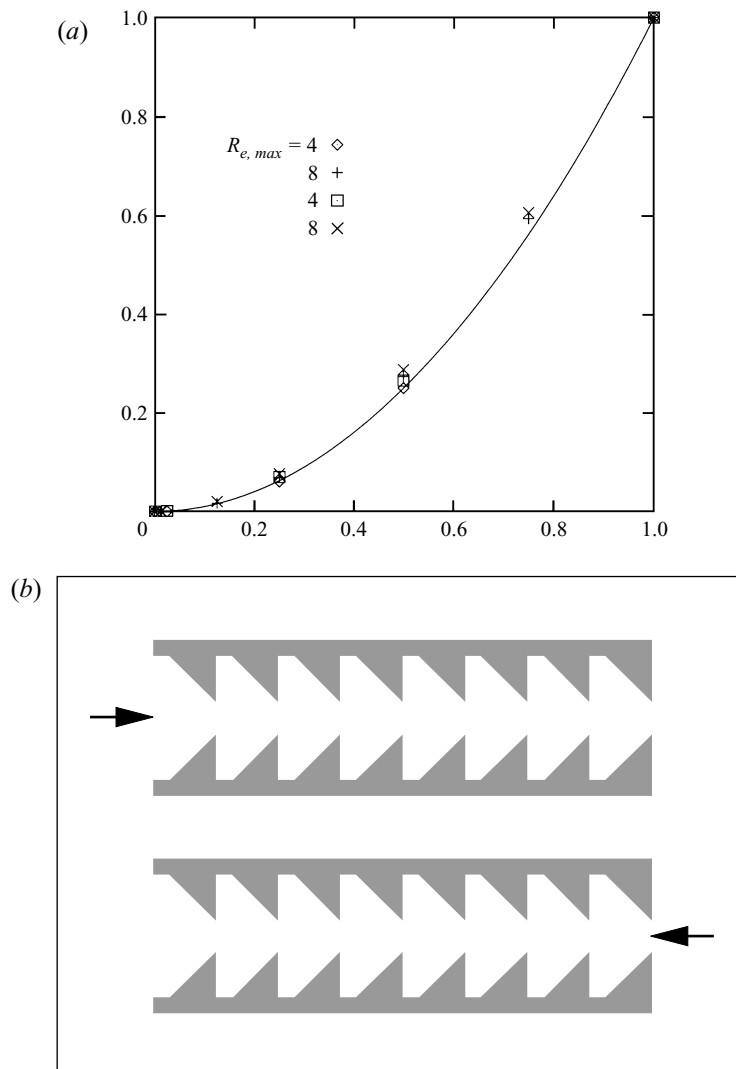
(a)

(b)

FIGURE 10. (*a*) Monodimensional case without flux reversibility. The curve is quadratic.
(*b*) Geometry of the periodic cell.

Figure 9(*b*) still concerns a rectangular cell for which $|\boldsymbol{t}_1|/|\boldsymbol{t}_2| = 2$. This cell is not invariant by central symmetry but we have verified numerically that it satisfies (H). The normalized deviation from Darcy's law for $\lambda = \mathrm{e}^{\mathrm{i}\pi/2}$ is presented in figure 9(*a*). Up to $R_{e,max} = 8$, the nonlinear correction is quadratic.

Figure 10(*b*) concerns a one-dimensional case corresponding to the sawtooth model G tested by Chauveteau. Though there is no reversibility of the seepage velocity (i.e. (H) is not satisfied), theorem 3.3 applies. The normalized deviation from Darcy's law in both directions is plotted in figure 10(*a*). The nonlinear correction is quadratic for all flow orientations up to $R_{e,max} = 8$.

Figure 11(*b*) shows a two-dimensional counterexample where (H) is not numerically satisfied (not an easy task). For $\lambda = \mathrm{e}^{\mathrm{i}5\pi/6}$ one can see in figure 11(*a*) that the normalized deviation to Darcy's law is linear in the Reynolds number. This case
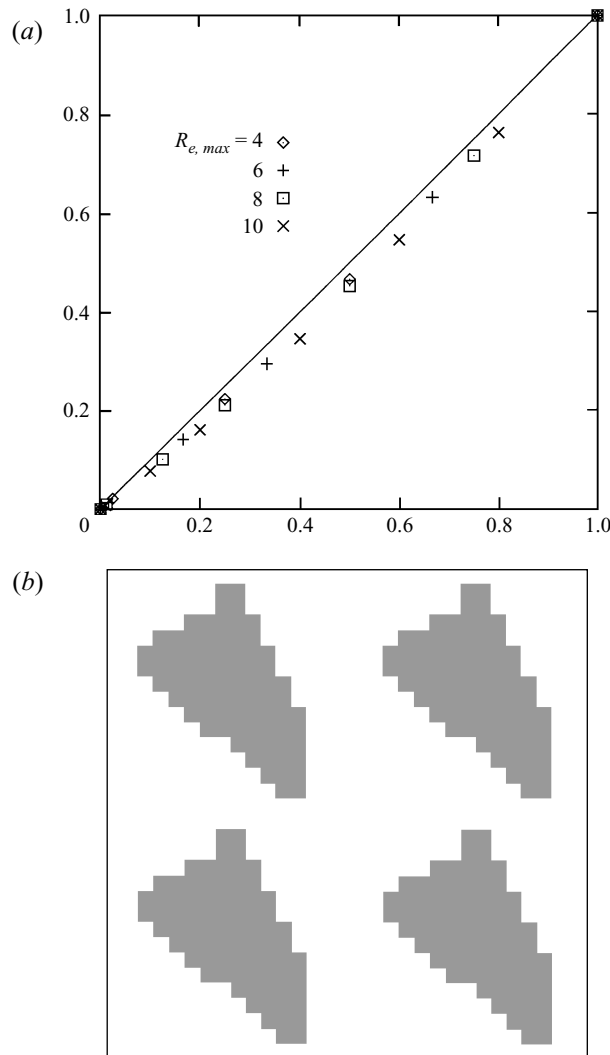
FIGURE 11. (*a*) Anisotropic case for which (H) is not satisfied. The curve is linear. (*b*) Geometry of the periodic cell.

suggests that in addition to being sufficient, hypothesis (H) may also be necessary; this, however, is still a conjecture which needs further investigation.

5. Conclusions

We have shown is this paper that under hypothesis (H) (which amounts to no assumption for one-dimensional filtration, or reversibility for two- and three-dimensional flows) the nonlinear correction to Darcy's law is quadratic in terms of the Reynolds number, and cubic with respect to the seepage velocity. This conclusion holds in practice if the data of the problem satisfy the condition (3.5). We have supported this claim by reinterpreting some well-known filtration experiments (by Darcy, Hazen, and Chauveteau). We have also provided a mathematical proof (restricted to unbounded periodic porous media) and have confirmed our theoretical results by numerical sim-

ulations. Still, from the mathematical point of view, the present work is not complete, since a rigorous theory for bounded porous media does not exist. For the mathematical aspects of hypothesis (H) in the context of the homogenization theory in bounded domains we refer to Bourgeat & Marušić-Paloka (1995) for one-dimensional flows and to Bourgeat, Marušić-Paloka & Mikelic (1996) for the multi-dimensional case.

REFERENCES

ALLAIRE, G. 1989 Homogenization of the Stokes flow in a connected porous medium. *Asymptotic Anal.* **2**, 203–222.

ARQUIS, E. & CALTAGIRONE, J.-P. 1984 Sur les conditions hydrodynamiques au voisinage d'un interface milieu fluide – milieu poreux: application à la convection naturelle. *C. R. Acad. Sci.* II **299**, 1–4.

BECKERMANN, C., RAMADHYANI, S. & VISKANTA, R. 1987 Natural convection flow and heat transfer between a fluid layer and a porous layer inside a rectangular enclosure. *Trans. ASME J. Heat Transfer* **109**, 363–370.

BENSOUSSAN, A., LIONS, J.-L. & PAPANICOLAOU, G. 1978 *Asymptotic Analysis for Periodic Structures.* North Holland.

BOURGEAT, A. & MARUŠIĆ-PALOKA, E. 1995 Loi d'écoulement non linéaire entre deux plaques ondulées. *C. R. Acad. Sci.* I **321**, 1115–1120.

BOURGEAT, A., MARUŠIĆ-PALOKA, E. & MIKELIC, A. 1996 Weak nonlinear corrections for Darcy's law. *M3AS* **8**, 6.

CHAUVETEAU, G. 1965 Essai sur la loi de Darcy. Thèse, Université de Toulouse.

DARCY, H. 1856 *Fontaines Publiques de la Ville de Dijon.* Librairie des Corps Impériaux des Ponts et Chaussées et des Mines, Paris.

FIRDAOUSS, M. & GUERMOND, J.-L. 1995 Sur l'homogénéisation des équations de Navier–Stokes à faible nombre de Reynolds. *C. R. Acad. Sci. Paris* I **320**, 245–251.

FORCHHEIMER, P. 1901 Wasserbewegung durch Boden. *Z. Vereines deutscher Ingnieure*, **XXXXV**, 49, 1736–1741, and 50, 1781–1788.

GIRAULT, V. & RAVIART, P.-A. 1986 *Finite Element Methods for Navier–Stokes Equations.* Springer.

HARLOW, F. H. & WELCH, F. E. 1965 Numerical calculation of time-dependent viscous incompressible flow of fluid with free surface. *Phys. Fluids* **8**, 2182–2189.

HAZEN, A. 1895 *The Filtration of Public Water-Supplies* Wiley.

LINDQUIST, E. 1930 In *Proceedings of Premier Congrès des Grands Barrages*, Stockholm.

MUSKAT, M. 1946 *The Flow of Homogeneous Fluids through Porous Media.* The Mapple Press Company, York, PA.

MEI, C. & AURIAULT, J.-L. 1991 The effect of weak inertia on flow through a porous medium. *J. Fluid Mech.* **222**, 647–663.

RASOLOARIJAONA, M. & AURIAULT, J.-L. 1994 Nonlinear seepage flow through a rigid porous medium. *Eur. J. Mech.* B/*Fluids* **13**, 177–195.

SANCHEZ-PALENCIA, E. 1980 *Non Homogeneous Media and Vibration Theory.* Lecture Notes in Physics. Springer.

TARTAR, L. 1980 Convergence of the homogenization process Appendix Sanchez-Palencia (1980).

WODIE, J.-C. & LEVY, T. 1991 Correction non linéaire de la loi de Darcy. *C. R. Acad. Sci. Paris* II **312**, 157–161.